An Alternative Form of Propagation Criterion for Two Collinear Cracks under Compression

ZHEMING ZHU
Department of Engineering Mechanics, Sichuan University, Chengdu, Sichuan, 610065, China

(Received 29 November 2007; 1 February 2008)

Abstract: Under compression, cracks extend, branch and coalesce. These fracturing processes have received much attention recently. In this paper, an attempt is made to find the analytical solution of stress intensity factors for the special case of cracks situated along a straight line, and to set up a fracture criterion. Under compression, cracks close and the crack surface friction can resist crack surface sliding. Considering crack surface friction, a set of complex stress functions is proposed for the special case of cracks situated along a straight line. The analytical solution is formulated, and for the case of only two collinear cracks inside an infinite plate, the exact analytical solution of stress intensity factor is presented. Finally, an alternative form of crack propagation criterion for two collinear cracks under compression is developed, which is expressed in terms of principal stresses. For the case of materials without pre-existing macrocracks, this new propagation criterion becomes the well known Coulomb–Mohr criterion.

Key Words: stress intensity factor, crack propagation criterion, crack surface friction, fracture toughness

1. INTRODUCTION

Most brittle materials in nature contain pre-existing cracks or flaws, such as underground rock mass and concrete, and they usually are subjected to compressive loadings. Therefore, in the study of crack propagation of brittle materials under compression, the following three aspects have to be considered:

(1) *The interaction effect between cracks.* The cracks inside a material affect each other, and under certain conditions, they extend, branch and coalesce. Recently, these fracturing processes have received the most attention [1–8]; however, no exact analytical solution is available as yet. The analytical solution is a critical step in our understanding of material fracturing.

(2) *Confining stress.* For cracked materials, the confining stress affects the crack tip stress intensity factors (SIFs) significantly, and the SIF values decrease as the confining stress increases [9, 10].

Mathematics and Mechanics of Solids **14:** 727–746, 2009 DOI: 10.1177/1081286508090043

Los Angeles, London, New Delhi and Singapore
Figures 4, 6 appears in color online: http://mms.sagepub.com

(3) *Crack surface friction.* Under compression, cracks close and friction exists between the crack surfaces. The friction can resist crack surface sliding and thus it significantly affects crack tip stress intensity factors [9].

For the problem of a single crack under compression, by using the boundary collocation method, Zhu et al. [9–13] and Xie et al. [14] presented analytical and numerical results, and the effects of crack surface friction and confining stress on crack SIF were analyzed. By using the analytical and numerical results, a new biaxial failure criterion for a single crack under compression was developed [10]. But they only considered a single crack in compression, thus their results cannot be directly applied to the case of multiple cracks under compression.

For the problem of a plate containing multiple collinear cracks, a number of researchers have implemented their studies theoretically. The solution for a plate containing two collinear cracks was first obtained by Willmore [15], and the particular case of a uniform pressure applied on the crack surfaces was considered. Muskelishvili [16] established and formulated the fundamental equations for solving the problem of an infinite plate containing collinear cracks by using complex stress functions. By mapping the crack plane on to a circular annulus and using the complex stress functions, Mikhlin [17] formulated the problem as a singular integral equation for the special case when the resultant of the external forces acting on the cracks are zero, and an approximate solution was presented. Erdogan [18] presented the solution in terms of complex stress functions for an infinite plate with two collinear cracks under the most general boundary conditions, but he did not consider compressive loadings which will cause cracks to close. Hori and Nemat-Nasser [19] proposed a pseudo-traction method to treat the general problems with any number of interacting cracks or other inhomogeneities. In the study of microcrack interaction with a finite main crack, Gong [20] formulated the stress intensity factor based on the assumption that crack surfaces are stress free. Wang [21] employed a boundary force method to solve the stress intensity factor for a rectangular plate with collinear cracks under uniaxial tension. But under compression, the cracks will close and the crack surfaces are not stress free, therefore, their solutions are not applicable to the case of cracks under compression. Chen et al. [22] proposed a variety of integral equations for the multiple-crack problem. Athough the problem of collinear cracks has been studied by the above researchers, and many significant results have been presented, however, the main focus for external loadings has been on tension and shear, and less attention has been paid to compression, which causes crack closing and crack surface friction. This paper will study the collinear-crack problem with particular emphasis on the issue of crack closing or the crack surface friction, and an alternative form of crack propagation criterion will be developed.

The general crack propagation criteria for mode II crack can be written as $K_{\mathrm{II}} \leq K_{\mathrm{IIC}}$, i.e. the stress intensity factor K_{II} is less than or equal to the material fracture toughness K_{IIC}. However, such propagation criterion is difficult to apply because K_{IIC} is difficult to measure, and the technique used in measuring fracture toughness is still not flawless, thus the measurement results are usually scattered in a large range. In order to avoid such difficulties in measuring fracture toughness, the general crack propagation criterion will be transformed into a new form expressed in terms of principal stresses, without K_{II} and K_{IIC} being involved.

Considering crack surface friction, a set of complex stress functions is proposed. For the general case of an infinite plate containing collinear cracks under compression, the an-

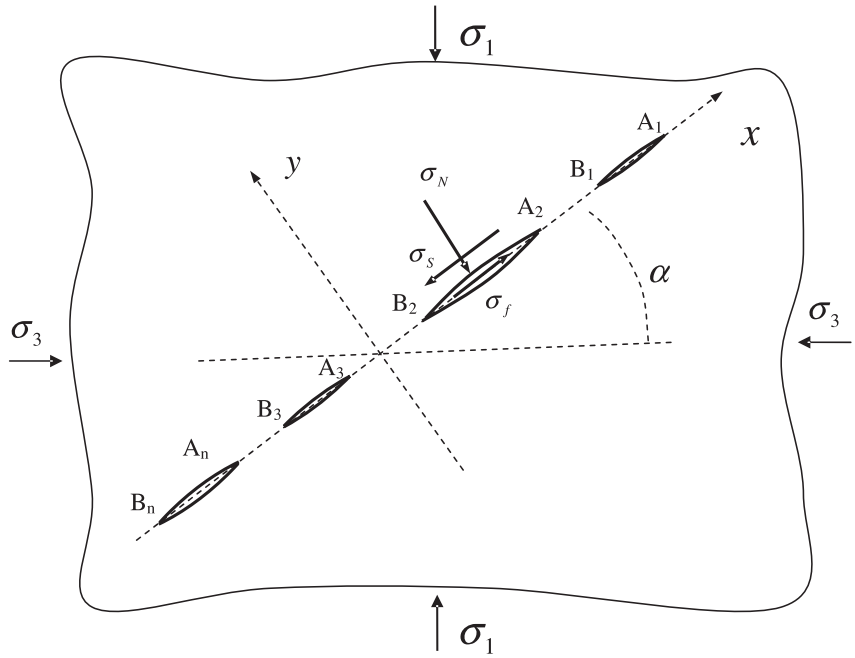

Figure 1. Sketch of an infinite plate containing a group of collinear cracks under compression, where $\sigma_{\mathrm{N}}\left(\sigma_{\mathrm{N}} = \frac{\sigma_1+\sigma_3}{2} + \frac{\sigma_1-\sigma_3}{2}\cos 2\alpha\right)$ is normal stress, $\sigma_{\mathrm{S}}\left(\sigma_{\mathrm{S}} = \frac{\sigma_1-\sigma_3}{2}\sin 2\alpha\right)$ is shear stress, and σ_{f} is the friction which is acting on the upper surfaces of crack $\mathrm{A_2B_2}$.

alytical solution is formulated; and for the case of only two collinear cracks, the exactly analytical solution of stress intensity factors is presented. By using the analytical solution, the influences of crack surface friction, confining stress, and the distance between two crack tips are analyzed. Finally, an alternative form of crack propagation criterion is developed for materials containing two collinear cracks under compression. In some special cases, this criterion can be simplified, and the results are very interesting. Especially, for the case of materials without pre-existing macrocracks, this criterion is identical with the well known Coulomb–Mohr criterion.

2. STRESS INTENSITY FACTOR FOR AN INFINITE PLATE CONTAINING COLLINEAR CRACKS IN COMPRESSION

Figure 1 shows an infinite plate subjected to far-field compressive principal stresses, σ_1 and σ_3, and a group of cracks are situated along a straight line, the x-axis. Suppose there are n cracks with ends a_k, b_k for $k = 1, 2, 3, \ldots, n$. Under compression, the cracks close and the crack surfaces are subjected to normal compressive stress σ_{N}, and friction σ_{f} (see Figure 1). The crack surface friction coefficient is f, and the angle between the crack and the σ_3-axis is α, which varies from 0° to 90°.

According to [16], for the elastic plane problem, the stresses can be expressed in terms of the complex stress functions, $\Phi(z)$ and $\Omega(z)$, as

$$\sigma_{xx} + \sigma_{yy} = 4\,\mathrm{Re}\,[\Phi(z)] \tag{1}$$

$$\sigma_{yy} - \mathrm{i}\sigma_{xy} = \Phi(z) + \Omega(\bar{z}) + (z - \bar{z})\overline{\Phi'(z)} \tag{2}$$

where $z = x + \mathrm{i}y$. The equilibrium equations and the compatibility conditions are automatically satisfied, and the resultant force boundary condition can be expressed as

$$\varphi(z) + \omega(\bar{z}) + (z - \bar{z})\overline{\Phi(z)} = \mathrm{i}\int_{z_0}^{z} (\bar{X} + \mathrm{i}\bar{Y})\mathrm{d}s + C_0 \tag{3}$$

where $\varphi(z) = \int \Phi(z)\mathrm{d}z$ and $\omega(z) = \int \Omega(z)\mathrm{d}z$, $\bar{X}$ and $\bar{Y}$ are the surface forces along the boundary in the x and y direction, respectively, and z_0 is an arbitrary point on the boundary. The positive direction of the integral is assumed such that the region always lies to the left. In Equation (3), the constant C_0 can be omitted, which will not affect the solutions of stresses and displacements. The displacement boundary condition can be expressed as

$$2G(u + \mathrm{i}v) = \kappa\varphi(z) - \omega(\bar{z}) - (z - \bar{z})\overline{\Phi(z)} \tag{4}$$

where $\kappa = (3-\nu)/(1+\nu)$ for plane stress and $\kappa = 3-4\nu$ for plane stress, $G = E/2(1+\nu)$, E is elastic modulus, and ν is Poisson's ratio. The stress boundary condition can be written as

$$\begin{aligned} \sigma_{xx} l + \tau_{xy} m &= X_n \\ \tau_{xy} l + \sigma_{yy} m &= Y_n \end{aligned} \tag{5}$$

where l and m are the direction cosines of the normal line of the boundary, and X_n and Y_n are the force components on the boundary. From Equation (5) and Figure 1, the crack surface stress conditions can be expressed as

$$\begin{aligned} (\sigma_{yy})^+ &= -\sigma_{\mathrm{N}}, \qquad (\sigma_{xy})^+ = -\sigma_{\mathrm{f}} \quad \text{(upper surface)} \\ (\sigma_{yy})^- &= -\sigma_{\mathrm{N}}, \qquad (\sigma_{xy})^- = -\sigma_{\mathrm{f}} \quad \text{(lower surface)} \end{aligned} \tag{6}$$

where σ_{f} and σ_{N} are the crack surface friction and the normal compressive stress, respectively (see Figure 1). Substituting Equation (6) into Equation (2), one has

$$\begin{aligned} (\sigma_{yy})^+ - \mathrm{i}(\sigma_{xy})^+ &= \Phi^+(t) + \Omega^-(t) = -\sigma_{\mathrm{N}} + \mathrm{i}\sigma_{\mathrm{f}} \\ (\sigma_{yy})^- - \mathrm{i}(\sigma_{xy})^- &= \Phi^-(t) + \Omega^+(t) = -\sigma_{\mathrm{N}} + \mathrm{i}\sigma_{\mathrm{f}} \end{aligned}$$

or

$$\begin{aligned}[\Phi(t)+\Omega(t)]^{+}+[\Phi(t)+\Omega(t)]^{-} &= -2\sigma_{\mathrm{N}}+2\mathrm{i}\sigma_{\mathrm{f}}=Q\\ [\Phi(t)-\Omega(t)]^{+}-[\Phi(t)-\Omega(t)]^{-} &= 0\end{aligned} \tag{7}$$

where Q is a constant. This is a simple Hilbert problem.

If the shear stress σ_{S} $\left(\sigma_{\mathrm{S}}=\frac{\sigma_1-\sigma_3}{2}\sin 2\alpha\right)$, which is parallel to the crack surface (see Figure 1), is less than the crack surface friction, i.e. $\sigma_{\mathrm{S}}<\sigma_{\mathrm{N}}f$, where $\sigma_{\mathrm{N}}=\frac{\sigma_1+\sigma_3}{2}+\frac{\sigma_1-\sigma_3}{2}\cos 2\alpha$, then the crack tip stress intensity factor is zero because large crack surface friction will result in a crack tip without stress concentration; only when $\sigma_{\mathrm{S}}\geq\sigma_{\mathrm{N}}f$ does the crack tip stress intensity factor exist, and in this case σ_{f} can be written as

$$\sigma_{\mathrm{f}}=\sigma_{\mathrm{N}}f=\left(\frac{\sigma_1+\sigma_3}{2}+\frac{\sigma_1-\sigma_3}{2}\cos 2\alpha\right)f. \tag{8}$$

Therefore, the constant Q in Equation (7) can be obtained:

$$Q=(-1+\mathrm{i}f)[\sigma_1+\sigma_3+(\sigma_1-\sigma_3)\cos 2\alpha] \tag{9}$$

For the problem of multiple cracks shown in Figure 1, the Plemelj function can be written as

$$X(z)=\sqrt{(z-a_1)(z-b_1)(z-a_2)(z-b_2)\cdots(z-a_n)(z-b_n)}. \tag{10}$$

It can be seen that as $z\to\infty$, $z^{-n}X(z)\to 1$, and on the crack surfaces, $X^{+}(t)=-X^{-}(t)$, where t is the coordinate of a point on the crack surface. According to [16, 18, 23], for the infinite plate under compression, the above Hilbert problem can be formulated as follows:

$$\Phi(z) = \frac{1}{4\pi\mathrm{i}X(z)}\int_L\frac{X^{+}(t)Q\mathrm{d}t}{(t-z)}+\frac{P(z)}{X(z)}-\frac{1}{2}\bar{\Gamma}' \tag{11}$$

$$\Omega(z) = \frac{1}{4\pi\mathrm{i}X(z)}\int_L\frac{X^{+}(t)Q\mathrm{d}t}{(t-z)}+\frac{P(z)}{X(z)}+\frac{1}{2}\bar{\Gamma}' \tag{12}$$

where $P(z)=k_0+k_1z+k_2z^2+\cdots+k_nz^n$

$$\begin{aligned}\Gamma &= -\frac{1}{4}(\sigma_1+\sigma_3)\\ \bar{\Gamma}' &= \frac{1}{2}(\sigma_1-\sigma_3)\mathrm{e}^{2\mathrm{i}(\frac{\pi}{2}-\alpha)}\\ k_n &= \Gamma+\frac{1}{2}\bar{\Gamma}'=-\frac{\sigma_1+\sigma_3}{4}-\frac{\sigma_1-\sigma_3}{4}(\cos 2\alpha-\mathrm{i}\sin 2\alpha)\end{aligned}$$

where $L=L_1+L_2+L_3+\cdots+L_n$ is the union of the n cracks, $k_0,k_1,k_2,\ldots,k_n$ are constants, and σ_1, σ_3 and α are shown in Figure 1. The integrals along L in Equations (11)

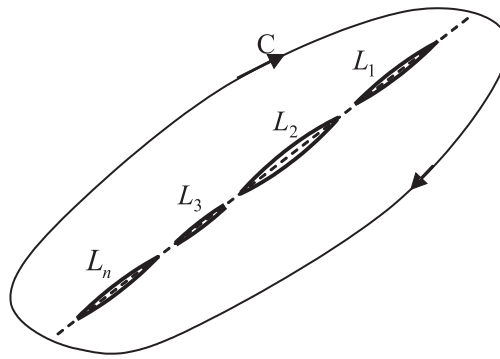

Figure 2. Sketch of a group of collinear cracks and a lacet surrounding these cracks.

and (12) can be expressed in terms of integrals along a lacet C surrounding these cracks as shown in Figure 2 (for this transformation, see [18,23]), and then Equation (11) can be rewritten as

$$\Phi(z) = \frac{Q}{8\pi \mathrm{i} X(z)} \int_C \frac{X(\varsigma)\mathrm{d}\varsigma}{(\varsigma - z)} + \frac{k_0 + k_1 z + k_2 z^2 + \cdots + k_n z^n}{X(z)} - \frac{1}{2}\bar{\Gamma}'. \tag{13}$$

By using residue theory, the integral in Equation (13) along contour C can be expressed in terms of the sum of the residues at point z and at infinity, thus Equation (13) can be expressed as

$$\Phi(z) = \frac{Q}{4X(z)} \left\{ X(z) + \mathrm{Res}\left[\frac{X(\varsigma)}{\varsigma - z}, \infty\right] \right\} + \frac{k_0 + k_1 z + k_2 z^2 + \cdots + k_n z^n}{X(z)} - \frac{1}{2}\bar{\Gamma}'. \tag{14}$$

If the above residues can be solved and the n coefficients, $k_0, k_1, k_2, \ldots, k_n$, are known, the complete solution of $\Phi(z)$ can be obtained.

As the infinite plane contains n cracks, the n coefficients, $k_0, k_1, k_2, \ldots, k_n$, must be chosen so that the displacement field is single-valued, i.e. non-dislocation. The conditions of single-valued displacements are

$$\kappa \int_{C_k} \Phi(z)\mathrm{d}z - \int_{C_k} \Omega(\bar{z})\mathrm{d}\bar{z} = 0 \quad (k = 1, 2, 3, \ldots, n) \tag{15}$$

where C_k is the contour of the kth crack. If the contour C_k shrinks to a lacet around the crack, Equation (15) can be rewritten as

$$\kappa \int_{L_k} [\Phi^+(t) - \Phi^-(t)]\mathrm{d}t - \int_{L_k} [\Omega^-(t) - \Omega^+(t)]\mathrm{d}t = 0 \quad (k = 1, 2, 3, \ldots, n) \tag{16}$$

where t is the coordinate of a point on the crack surface. Applying this condition for $k = 1, 2, 3, \ldots, n$ yields n linear equations for the determination of the n coefficient. There-

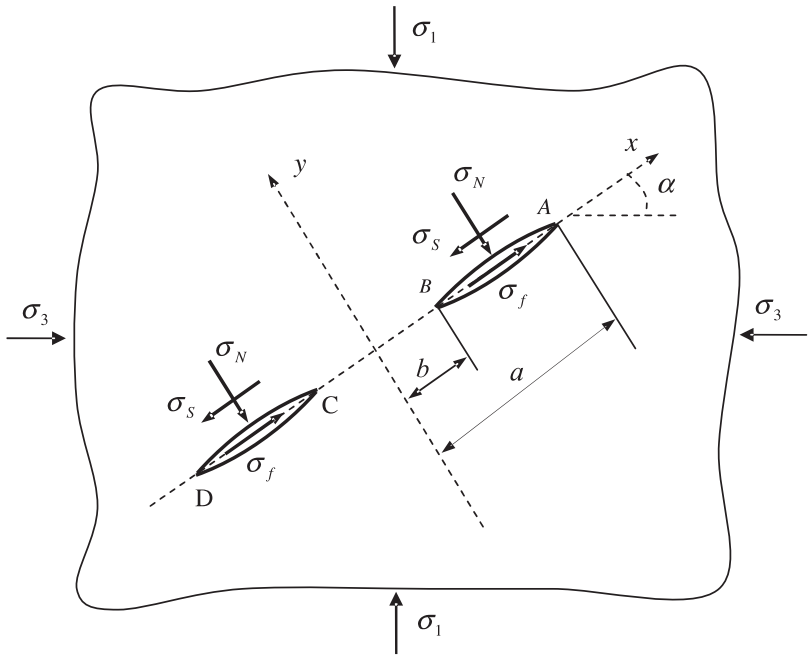

Figure 3. Sketch of an infinite plate containing two collinear cracks under compression, where σ_{N} $\left(\sigma_{\mathrm{N}} = \frac{\sigma_1+\sigma_3}{2} + \frac{\sigma_1-\sigma_3}{2}\cos 2\alpha\right)$ is normal stress, σ_{S} $\left(\sigma_{\mathrm{S}} = \frac{\sigma_1-\sigma_3}{2}\sin 2\alpha\right)$ is shear stress, and σ_{f} is the friction which is acting on the upper crack surfaces.

fore, for an infinite plate containing finite collinear cracks under compression, one may theoretically obtain the stress functions $\Phi(z)$ and $\Omega(z)$ from Equations (14) and (16). However, because the stress functions contain the Plemelj function $X(z)$, the process of solving the n coefficients may be difficult due to the high-order elliptic integrals involved.

3. SOLUTION FOR TWO COLLINEAR CRACKS UNDER COMPRESSION

For an infinite plate containing two collinear cracks as shown in Figure 3, the above equations can be simplified. Suppose the two cracks are symmetrical about the origin, and the lengths of the two cracks are the same and equal to $a - b$. The corresponding Plemelj function can be simplified as

$$X(z) = \sqrt{(z^2 - a^2)(z^2 - b^2)} \tag{17}$$

and the corresponding polynomial $P(z)$ can be simplified as $P(z) = k_0 + k_1 z + k_2 z^2$, where $k_2 = k_n$. In this case, Equation (14) can be solved and $\Phi(z)$ can be expressed as

$$\Phi(z) = \frac{Q}{4} - \frac{Q(2z^2 - a^2 - b^2)}{8X(z)} + \frac{k_0 + k_1 z + k_2 z^2}{X(z)} - \frac{\sigma_1 - \sigma_3}{4} e^{i(\pi - 2\alpha)}. \tag{18}$$

Because the loadings and cracks are symmetrical about the origin, the constant k_1 in the above equations must be zero. Substituting Equation (9) into Equation (18), $\Phi(z)$ can be rewritten as

$$\Phi(z) = \frac{k_0 + S_0 + Sz^2}{X(z)} - \frac{(1 - if)(\sigma_1 + \sigma_3)}{4} + i\frac{\sigma_1 - \sigma_3}{4}(f \cos 2\alpha - \sin 2\alpha) \tag{19}$$

where

$$\begin{aligned} S_0 &= \frac{if - 1}{8}(a^2 + b^2)[\sigma_1 + \sigma_3 + (\sigma_1 - \sigma_3)\cos 2\alpha] \\ S &= -\frac{i}{4}[(\sigma_1 + \sigma_3)f + (\sigma_1 - \sigma_3)(f \cos 2\alpha - \sin 2\alpha)]. \end{aligned} \tag{20}$$

It can be seen that only one coefficient k_0 in Equation (19) is unknown. Similarly, from Equation (12), the function $\Omega(z)$ can be obtained:

$$\begin{aligned} \Omega(z) &= \frac{k_0 + S_0 + Sz^2}{X(z)} - \frac{(1 - if)(\sigma_1 + \sigma_3)}{4} \\ &+ \frac{\sigma_1 - \sigma_3}{4}[-2\cos 2\alpha + i(f \cos 2\alpha + \sin 2\alpha)]. \end{aligned} \tag{21}$$

Substituting Equations (19) and (21) into Equation (16), for crack AB (Figure 3), one can have

$$2(\kappa + 1)\int_b^a \frac{k_0 + S_0 + St^2}{\sqrt{(t^2 - a^2)(t^2 - b^2)}} dt = 0. \tag{22}$$

Equation (22) can be split into two terms:

$$\int_b^a \frac{k_0 + S_0}{\sqrt{(t^2 - a^2)(t^2 - b^2)}} dt + \int_b^a \frac{St^2}{\sqrt{(t^2 - a^2)(t^2 - b^2)}} dt = 0. \tag{23}$$

Equation (23) contains two elliptic integrals, for which readers are referred to [24]. By solving the elliptic integrals, the constant k_0 is obtained:

$$k_0 = -a^2 S\frac{E(m)}{K(m)} - S_0 \tag{24}$$

where $K(m)$ and $E(m)$ are complete elliptic integrals of the first and second kinds, respectively, and $m = 1 - \frac{b^2}{a^2}$. According to [24], the value of $E(m)/K(m)$ can be evaluated by

$$\frac{E(m)}{K(m)} = \frac{1 - \left(\frac{1}{2}\right)^2 \frac{m}{1} - \left(\frac{1}{2}\cdot\frac{3}{4}\right)^2 \frac{m^2}{3} - \left(\frac{1}{2}\cdot\frac{3}{4}\cdot\frac{5}{6}\right)^2 \frac{m^3}{5} - \cdots}{1 + \left(\frac{1}{2}\right)^2 m + \left(\frac{1}{2}\cdot\frac{3}{4}\right)^2 m^2 + \left(\frac{1}{2}\cdot\frac{3}{4}\cdot\frac{5}{6}\right)^2 m^3 + \cdots}. \tag{25}$$

Substituting Equation (24) into Equation (19), $\Phi(z)$ can be rewritten as

$$\Phi(z) = \frac{S}{X(z)}\left[z^2 - a^2\frac{E(m)}{K(m)}\right] - \frac{(1 - \mathrm{i}f)(\sigma_1 + \sigma_3)}{4} + \mathrm{i}\frac{\sigma_1 - \sigma_3}{4}(f\cos 2\alpha - \sin 2\alpha). \tag{26}$$

The stress intensity factors (SIFs) can be calculated by

$$K_{\mathrm{I}} - \mathrm{i}K_{\mathrm{II}} = \lim_{z\to ct} 2\sqrt{2\pi(z - ct)}\Phi(z) = \lim_{z\to ct}\frac{2\sqrt{2\pi(z - ct)}\cdot S}{\sqrt{(z^2 - a^2)(z^2 - b^2)}}\left[z^2 - a^2\frac{E(m)}{K(m)}\right] \tag{27}$$

where K_{I} and K_{II} are the SIFs of mode I and mode II, respectively, and ct is the x-coordinate of crack tips (at crack tip A, $ct = a$). Because the coefficient S is a pure imaginary function in Equation (20), the mode I factor K_{I} is zero, which corresponds to the real value of the complex function in the right-hand side of Equation (27). It should be noted that after propagation, wing-cracks will develop, and the crack model will change from Mode II only to the mixed model of Mode I and Mode II.

From Equation (27), the dimensionless K_{II}, i.e. Y_{II}, at crack tip A (or D) and B (or C) can be expressed as

$$Y_{\mathrm{II}}^{\mathrm{A}} = \frac{K_{\mathrm{II}}}{K_0} = \frac{2Sa^{1.5}\mathrm{i}}{\sigma_1(a - b)\sqrt{(a + b)}}\left[1 - \frac{E(m)}{K(m)}\right] \tag{28}$$

$$Y_{\mathrm{II}}^{\mathrm{B}} = \frac{-2S\mathrm{i}}{\sigma_1(a - b)\sqrt{b(a + b)}}\left[b^2 - a^2\frac{E(m)}{K(m)}\right] \tag{29}$$

where $K_0 = \sigma_1\sqrt{\pi(a - b)}$, the coefficient S is presented in Equation (20), $E(m)/K(m)$ is presented in Equation (25), and the coefficients a, b, and σ_1 are shown in Figure 3.

It should be noted that the shear stress σ_{S} in Figure 3 $\left(\sigma_{\mathrm{S}} = \frac{\sigma_1 - \sigma_3}{2}\sin 2\alpha\right)$, which is parallel to the crack surface, must be larger than the crack surface friction, $\sigma_{\mathrm{N}}f$, i.e.

$$\frac{\sigma_1 - \sigma_3}{2}\sin 2\alpha > \left(\frac{\sigma_1 + \sigma_3}{2} + \frac{\sigma_1 - \sigma_3}{2}\cos 2\alpha\right) f. \tag{30}$$

Otherwise, the SIF is zero due to large crack surface friction and Equation (30) can be rewritten as

$$\frac{\sigma_3}{\sigma_1} < \frac{1 - f\cot\alpha}{1 + f\tan\alpha}. \tag{31}$$

Therefore, before applying Equations (28) or (29), one should use Equation (31) to examine if the crack SIF is zero, and if Equation (31) is not satisfied (that means $\sigma_{\mathrm{S}} \le \sigma_{\mathrm{N}}f$), the crack tip SIF is zero, i.e. $Y_{\mathrm{II}}^{\mathrm{A}} = Y_{\mathrm{II}}^{\mathrm{B}} = 0$.

Because $\frac{\sigma_3}{\sigma_1} \geq 0$, from Equation (31), one can have

$$1 - f \cot \alpha \geq 0, \quad \text{or} \quad \tan \alpha \geq f. \tag{32}$$

This means that $\tan \alpha$ should be larger than crack surface friction coefficient f, otherwise, the corresponding crack SIF must be zero.

4. CALCULATION RESULTS AND DISCUSSIONS

The calculation results show that the Mode II factors, K_{II}, are negative. The negative sign of K_{II} only expresses the direction of the wing-crack propagation. Therefore, the negative sign of K_{II} (or Y_{II}) is disregarded, and only the magnitudes of K_{II} (or Y_{II}) are investigated in this paper.

4.1. Influence of Crack Surface Friction on Stress Intensity Factors

In this study, the calculation model is an infinite plate containing two collinear cracks as shown in Figure 3, the employed parameter a is 1.5 m and b is 0.5 m (thus the crack length is a constant, i.e. $a - b = 1.0$ m), and the ratio of σ_3/σ_1 is 0.2. The calculation results from Equations (28) and (29) are plotted in Figure 4. It can be seen that the difference between the values of the dimensionless K_{II}, i.e. Y_{II} ($Y_{\text{II}} = K_{\text{II}}/\sigma_1\sqrt{\pi\,(a-b)}$), at crack tip A and B are very small; at tip B they are slightly larger than those at tip A. The Y_{II} values at both tips decrease as the crack surface friction coefficient f increases. This is because friction resists crack surfaces sliding and thus reduces crack tip SIF. Similar results have been obtained from a finite plate containing a single crack [9] and from the photoelastic fringe results [25]. When the friction coefficient f is larger than 0.9, the corresponding $Y_{\text{II}}-\alpha$ curves merge into the α-axis. This means that a large crack surface friction could result in the crack tip being SIF-free. It can be seen that each curve in Figure 4 has a maximum value of Y_{II}. The angle α_m which corresponds to the maximum value of Y_{II} is called "the most unfavorable crack orientation". The values of α_m at crack tip A and B are the same, and α_m increases as f increases (Figure 4).

4.2. Influence of Confining Stress on Stress Intensity Factors

In this study the calculation model is an infinite plate containing two collinear cracks as shown in Figure 3, the employed parameters a is 1.5 m, b is 0.5 m, f is 0.2, and the ratio of σ_3/σ_1 varies from 0 to 1.0. The calculation results are plotted in Figure 5. It can be seen that the values of Y_{II} ($Y_{\text{II}} = K_{\text{II}}/\sigma_1\sqrt{\pi\,(a-b)}$) decrease as the confining stress increases. When σ_3/σ_1 is zero, the corresponding $Y_{\text{II}} - \alpha$ curve is the uppermost of all the curves, and when σ_3/σ_1 is larger than 0.7, all the $Y_{\text{II}} - \alpha$ curves merge into the α-axis.

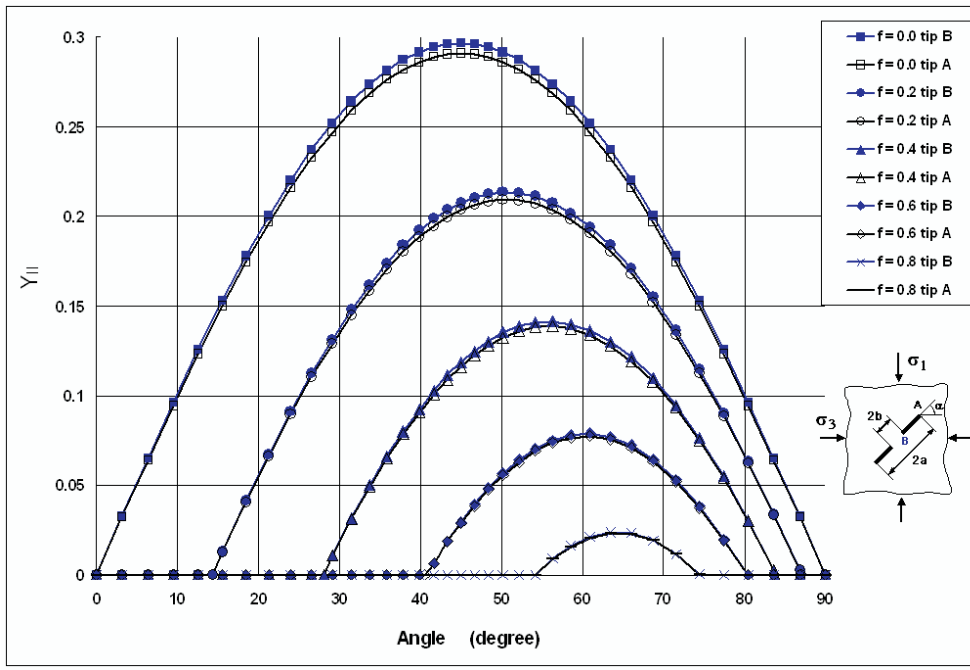

Figure 4. Curves of the magnitude of Y_{II} ($K_{II}/\sigma_1\sqrt{\pi(a-b)}$) versus α for an infinite plate containing two collinear cracks in compression (a = 1.5 m, b = 0.5 m, $\sigma_3/\sigma_1 = 0.2$), obtained from Equations (28) and (29); illustrating the influence of crack surface friction on stress intensity factors; the crack surface friction coefficient f varies from 0 to 0.8.

4.3. Influence of the Distance Between the Two Crack Tips on Stress Intensity Factors

In this study, the calculation model is shown in Figure 3, and the employed parameters friction coefficient f is 0.2, crack length, i.e. $a-b$, is 1.0 m, the angle α is 45°, and σ_3/σ_1 is 0.2. Figure 6 shows the calculation results for the relationship of Y_{II} versus $2b$, the distance between the two crack tips. In this calculation, $2b$ varies from 0.0 to 6.0 m. It should be noted when $2b$ equals zero, these two cracks will merge into one crack, and in this case only the SIF at crack tip A exists.

For the infinite plate, as $2b$ decreases from 6.0 m to 0.5 m, the Y_{II} values at both crack tip A and B increase slightly; as $2b$ decreases from 0.5 m to 0.0 m, the Y_{II} values at tip B increase rapidly. As $2b$ approaches zero, the Y_{II} values at tip B becomes a large value (e.g. when $2b = 0.0001$ m, $Y_{II} = 9.96$). This is due to the influence of the adjacent crack.

Figure 6 also presents the curves of Y_{II} versus $2b$ for a finite plate (size is 10 m × 10 m), obtained by using boundary collocation method [11–14]. It can be seen that as $2b$ increases from 1.75 m to 6.0 m, the Y_{II} values at both crack tip A and B increase obviously. This is because, for the finite plate, the cracks near the outer boundary are largely affected by the outer boundary and thus have high SIF values. Comparing with the infinite plate case, it can be seen that "confining" can significantly affect crack stabilities. At crack tip B, as $2b$

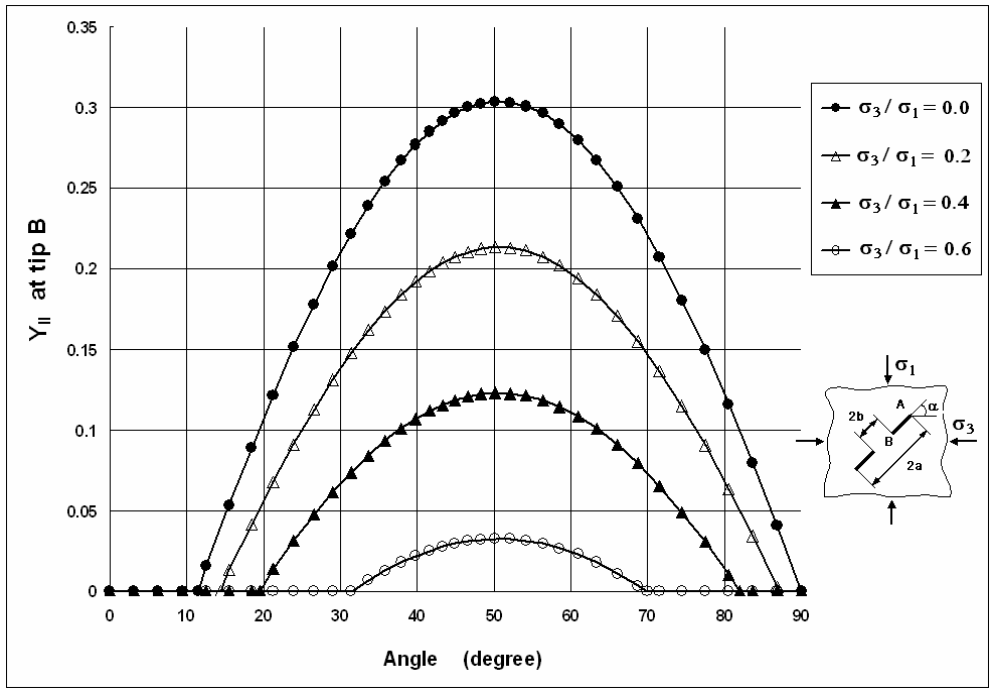

Figure 5. Curves of the magnitude of Y_{II} ($K_{II}/\sigma_1\sqrt{\pi(a-b)}$) versus α for an infinite plate containing two collinear cracks in compression (a = 1.5 m, b = 0.5 m, $f = 0.2$), obtained from Equation (29), illustrating the influence of confining stress on stress intensity factors; the ratio of σ_3/σ_1 varies from 0 to 1.0, but when it is larger than 0.7, all the Y_{II} values equal zero.

decreases from 1.75 m to 0.0 m, the Y_{II} values increase rapidly. As $2b$ approaches zero, Y_{II} at tip B tends towards a very large value (e.g. $2b = 0.0001$ m, $Y_{II} = 76.37$).

5. A PROPAGATION CRITERION FOR TWO COLLINEAR CRACKS UNDER COMPRESSION

From the above analyses, it can be seen that the crack surface frictions, the confining stresses and the distances between two crack tips affect the stress intensity factors significantly, and thus they affect material fracture behavior.

As is well known, the crack propagation criterion for mode II crack can be written as

$$K_{II} = Y_{II}\sigma_1\sqrt{\pi\ (a-b)} \leq K_{IIC} \tag{33}$$

where $a - b$ is crack length (see Figure 3), K_{IIC} is material fracture toughness, and Y_{II} can be obtained from Equation (29). From Figures 4–6 it can be seen that the values of Y_{II} (or K_{II})

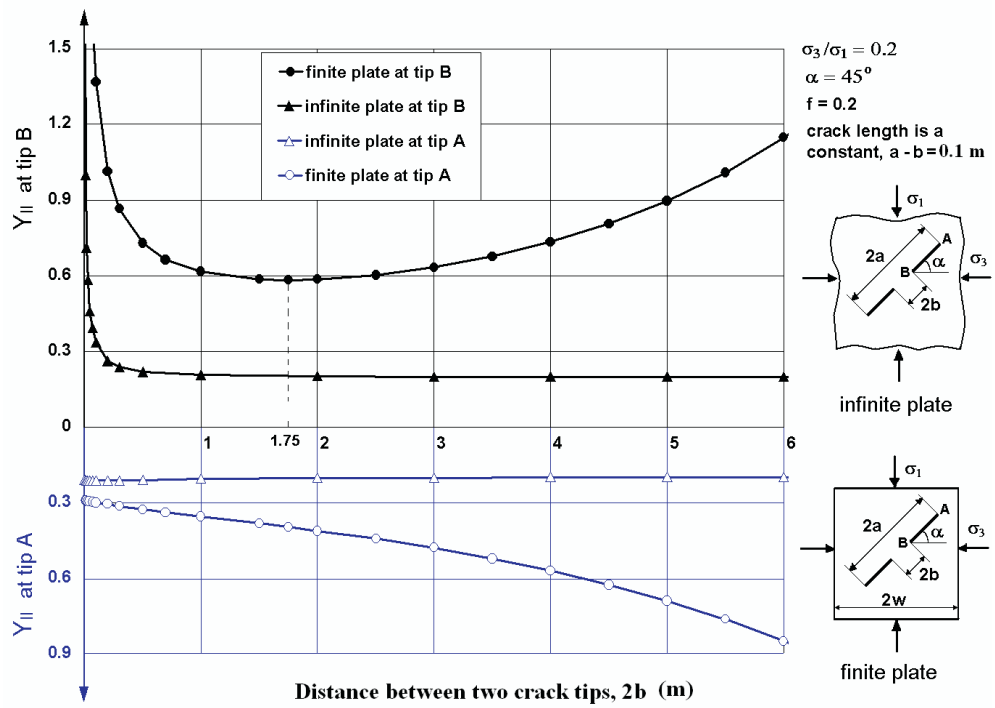

Figure 6. Curves of the magnitude of Y_{II} ($K_{II}/\sigma_1\sqrt{\pi(a-b)}$) versus $2b$ for an infinite plate and a finite plate containing two collinear cracks under compression, illustrating the influence of the distance between the two crack tips on stress intensity factors.

at tip B are larger than those at tip A; therefore, the values of Y_{II} at tip B, i.e. Equation (29), should be employed in Equation (33).

The crack propagation criterion, Equation (33), is difficult to apply because the fracture toughness generally is difficult to measure. The technique used in measuring material fracture toughness is still not flawless, and the measurement results are usually scattered in a large range, especially for brittle materials. In order to avoid such difficulties in measuring material fracture toughness, Equation (33) will be transformed into a new form expressed in terms of principal stresses, without K_{II} and K_{IIC} involved.

Considering a specimen containing two cracks under uniaxial compression as shown in Figure 7(a), its critical stress is σ_U, and the corresponding Y_{II} can be obtained from Equation (29) by substituting S from Equation (20) and taking $\sigma_3 = 0$:

$$Y_{II}^{B} = -\frac{f + f\cos 2\alpha - \sin 2\alpha}{2(a-b)\sqrt{b(a+b)}}\left[b^2 - a^2\frac{E(m)}{K(m)}\right]. \tag{34}$$

It should be noted that the value of Y_{II}^{B} in Equation (34) is negative. The absolute values of K_{II} can be written as

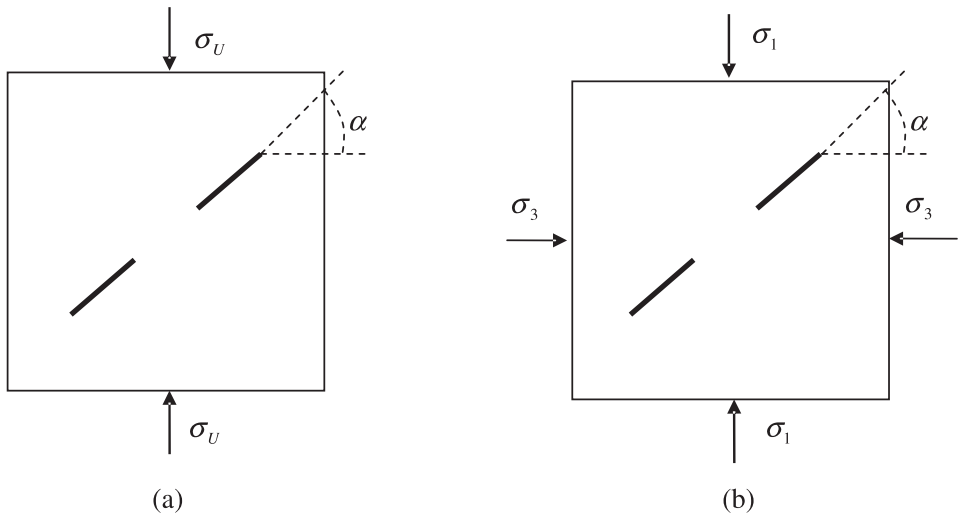

Figure 7. A specimen containing two inclined cracks under (a) uniaxial compression and (b) biaxial compression.

$$\begin{aligned} K_{\mathrm{II}} &= Y_{\mathrm{II}}^{\mathrm{B}} \sigma_U \sqrt{\pi (a-b)} \\ &= \frac{\sigma_{\mathrm{U}}(f + f\cos 2\alpha - \sin 2\alpha)}{2(a-b)\sqrt{b(a+b)}} \left[b^2 - a^2 \frac{E(m)}{K(m)} \right] \sqrt{\pi (a-b)}. \end{aligned} \tag{35}$$

Under the critical condition, the relation between K_{II} and K_{IIC} can be written as

$$K_{\mathrm{II}} = K_{\mathrm{IIC}}. \tag{36}$$

Substituting Equation (35) into Equation (36), one can have

$$\frac{\sigma_{\mathrm{U}}(f + f\cos 2\alpha - \sin 2\alpha)}{2(a-b)\sqrt{b(a+b)}} \left[b^2 - a^2 \frac{E(m)}{K(m)} \right] \sqrt{\pi (a-b)} = K_{\mathrm{IIC}}. \tag{37}$$

When the confining stress σ_3 is applied on this specimen as shown in Figure 7(b), its critical stress will increase from σ_{U} to σ_1. The corresponding K_{II} can be written as

$$K_{\mathrm{II}} = Y_{\mathrm{II}}^{\mathrm{B}} \sigma_1 \sqrt{\pi\ (a-b)}. \tag{38}$$

Substituting $Y_{\mathrm{II}}^{\mathrm{B}}$ from Equation (29) into Equation (38), the absolute values of K_{II} can be written as

$$K_{\mathrm{II}} = \frac{(\sigma_1 + \sigma_3) f + (\sigma_1 - \sigma_3)(f\cos 2\alpha - \sin 2\alpha)}{2(a-b)\sqrt{b(a+b)}} \left[b^2 - a^2 \frac{E(m)}{K(m)} \right] \sqrt{\pi (a-b)}. \tag{39}$$

Substituting Equations (37) and (39) into Equation (33), one can have

$$(\sigma_1 + \sigma_3) f + (\sigma_1 - \sigma_3)(f \cos 2\alpha - \sin 2\alpha) \geq \sigma_U (f + f \cos 2\alpha - \sin 2\alpha). \tag{40}$$

It should be noted that Equations (37) and (39) both contain a negative term $b^2 - a^2 \frac{E(m)}{K(m)}$, thus the direction of the inequality is changed. From Equation (40), the crack propagation criterion for two collinear cracks under compression is obtained:

$$\sigma_1 \leq \sigma_U + \frac{1 + f \cdot \tan\alpha}{1 - f \cdot \cot\alpha} \sigma_3 \tag{41}$$

where the friction coefficient f and the angle α must satisfy Equation (32), i.e. $1 - f \cdot \cot\alpha > 0$. Equation (41) is an alternative form of crack propagation criterion for two collinear cracks under compression, derived from the general crack propagation criterion, Equation (33). This criterion is expressed in terms of principal stresses, without K_{II} and K_{IIC} being involved, which is more convenient in application. The critical stress σ_1 in Equation (41) is related to four parameters: confining stress σ_3, uniaxial compressive strength σ_U, crack orientation α, and crack surface friction coefficient f (see Figure 3). It should be noted that σ_U is different from the UCS which is used in Coulomb–Mohr failure criterion because the specimen used in measuring σ_U should contain two collinear inclined cracks (see Figure 7a).

Under the critical state, the relation between σ_1 and σ_3, from Equation (41), can be written as

$$\sigma_1 = \sigma_U + \frac{1 + f \cdot \tan\alpha}{1 - f \cdot \cot\alpha} \sigma_3. \tag{42}$$

If the parameters of σ_U, σ_3 and α are kept as constants, the relationship between the critical stress σ_1 and the fiction coefficient f is as plotted in Figure 8. It can be seen that σ_1 increases with the increase of f. This is to be expected, as crack surface friction can resist crack surface sliding, and thus can reduce crack tip SIF values.

If the parameters of σ_U, α, and f are kept as constants, the relation between the critical stress σ_1 and the confining stress σ_3 is as plotted in Figure 9. It can be seen that σ_1 increases as σ_3 increases; when $\sigma_3 = 0$, $\sigma_1 = \sigma_U$, and accordingly, Equation (41) becomes

$$\sigma_1 \leq \sigma_U. \tag{43}$$

Equation (43) is the propagation criterion of two collinear cracks under uniaxial compression. The traditional uniaxial failure criterion for materials without cracks is $\sigma_1 \leq$ UCS, which is similar to Equation (43), but because the specimens contain cracks, σ_U should be lower than the corresponding UCS. Below the straight line, i.e. $\sigma_1 = \sigma_U + \sigma_3 \tan\theta$ shown in Figure 3, the corresponding cracks are stable. Here $\tan\theta$ is the slope of the straight line, and $\tan\theta = \frac{1+f\cdot\tan\alpha}{1-f\cdot\cot\alpha}$.

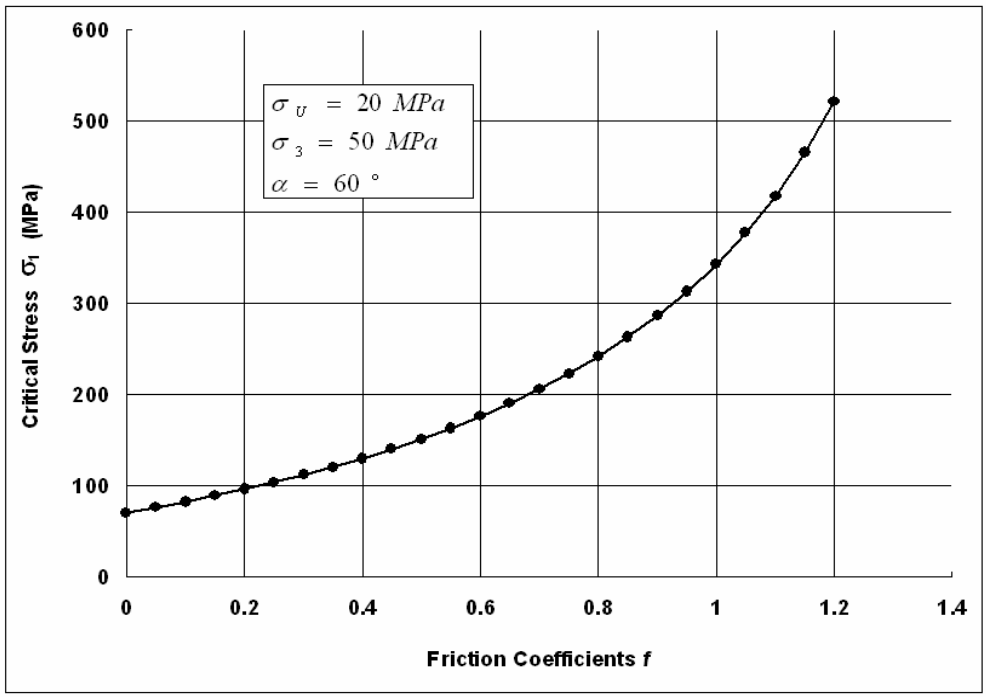

Figure 8. The relationship between the critical stress σ_1 and the fiction coefficients f when the parameters of σ_U, σ_3 and α are kept as constants; below the curve, the corresponding cracks are stable.

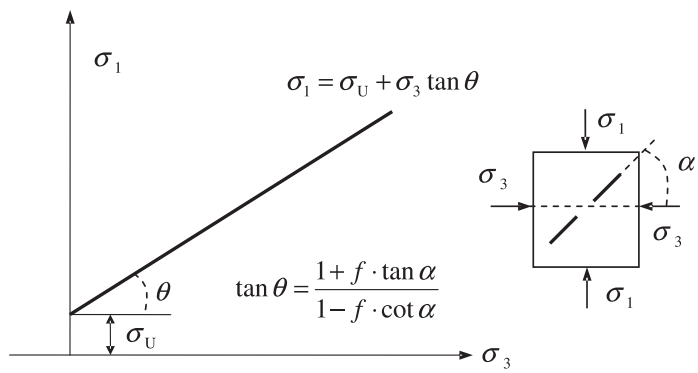

Figure 9. Sketch of the relationship between the critical stress σ_1 and the confining stress σ_3 when the parameters of σ_U, α and f are kept as constants; below the straight line, i.e. $\sigma_1 = \sigma_U + \sigma_3 \tan\theta$, the corresponding cracks are stable.

6. APPLICATIONS IN SOME SPECIAL CASES

In the following special cases, the crack propagation criterion can be simplified.

6.1. Crack Surface Friction Free

If the friction between crack surfaces is zero, i.e. $f = 0$, then Equation (41) becomes

$$\sigma_1 \leq \sigma_U + \sigma_3 \quad \text{or} \quad \sigma_1 - \sigma_3 \leq \sigma_U. \tag{44}$$

Equation (44) is similar to the traditional maximum shear stress failure criterion for materials without cracks. If σ_U is much less than σ_3, Equation (44) can be written as $\sigma_1 \leq \sigma_3$. Since σ_1 is never less than σ_3, then they must be equal, i.e. $\sigma_1 = \sigma_3$, which is the hydrostatic state of stress. This indicates that if there is no friction on crack surfaces, the corresponding crack stability is very low. Therefore, if cracks are filled with water, the crack stability will reduce.

6.2. For the Most Unfavorable Cracks

Differentiating Equation (39) with respect to α, and taking $K'_{II} = 0$, the orientation of the most unfavorable crack α_m is obtained:

$$\alpha_m = \frac{\pi}{2} - \frac{1}{2}\tan^{-1}\frac{1}{f}. \tag{45}$$

Because crack surface friction coefficient $f \geq 0$, and if $f = 0$, $\alpha_m = 45^\circ$, the orientation of the most unfavorable crack is never less than 45°. If $f = 1.0$, the orientation of the most unfavorable crack is 67.5°. For the most unfavorable crack, substituting Equation (45) into Equation (41), the relation between σ_1 and σ_3 can be rewritten as

$$\sigma_1 \leq \sigma_U + (\sqrt{1 + f^2} + f)^2\sigma_3. \tag{46}$$

It can be seen that for the most unfavorable crack, the critical stress σ_1 is only related to three parameters: confining stress σ_3, uniaxial compressive strength σ_U, and crack surface friction coefficient f.

6.3. Materials without Pre-existing Macrocracks

Brittle materials contain randomly distributed microcracks. If there are no pre-existing macrocracks, the fracture process will be governed by the most unfavorable microcracks, which will first start to propagate and cause the brittle materials to failure. Therefore, for materials without pre-existing macrocracks under compression, Equation (46) can be adopted as the crack propagation criterion.

For brittle materials without pre-existing macrocracks under compression, the sliding friction between the microcrack surfaces is the same as the internal friction defined by Coulomb [26, 27], i.e. $f = \mu = \tan\phi$, where μ is the internal friction coefficient, and

ϕ is the angle of internal friction defined by Coulomb. The well known Coulomb–Mohr failure criterion can be written as

$$\sigma_1 \leq \mathrm{UCS} + \sigma_3(\sqrt{1+\mu^2}+\mu)^2, \tag{47}$$

or in another form, $\tau \leq \mathrm{UCS} + \sigma \tan\phi$, which is more familiar for readers. For materials without pre-existing macrocracks, evidently $\sigma_U = \mathrm{UCS}$, then comparing Equation (47) with Equation (46), it can be seen that this crack propagation criterion for materials without pre-existing macrocracks is just the well known Coulomb–Mohr criterion.

7. CONCLUSIONS

Recently, the study of multiple-crack fracture behavior under compression has received much attention. This paper has implemented the theoretical study on the special case that cracks are situated along a straight line. The influences of crack surface friction, confining stress and the interaction between cracks on crack tip stress intensity factors have been investigated. For an infinite plate containing collinear cracks under compression, the solution of stress intensity factors has been formulated, and for the case of only two collinear cracks, exact analytical solution of the stress intensity factors is presented in Equations (28) and (29), which have been employed to establish an alternative form of crack propagation criterion.

The propagation criterion for two collinear cracks under compression, presented in this paper, is derived from the traditional fracture criterion, Equation (33), and is expressed in terms of principal stresses, without stress intensity factor and fracture toughness involved, which is easy to understand and apply. This propagation criterion is very useful because in nature many materials contain pre-existing cracks or flaws, and are subjected to compressive loadings. For the case of materials without pre-existing macrocracks, this criterion becomes the well known Coulomb–Mohr failure criterion.

Further theoretical studies on the topic of the fracturing behavior of multiple cracks under compression are necessary. For the case when cracks are distributed randomly, analytical solutions are imperative.

LIST OF SOME IMPORTANT SYMBOLS

a = the distance from crack tip A to the origin shown in Figure 3;

b = the distance from crack tip B to the origin shown in Figure 3;

a_k, b_k = crack tip coordinates of the kth crack ($k = 1, 2, 3, \ldots, n$);

C = a contour surrounding the n cracks shown in Figure 2;

C_k = a contour surrounding the kth crack;

$E(m)$ = the second kind of elliptic integral;

f = crack surface friction coefficient;

$L = L_1 + L_2 + L_3 + \cdots + L_n$ is the union of the n cracks;

$K(m)$ = the first kind of elliptic integral;

$k_0, k_1, k_2, \ldots, k_n$ = constants;

K_{II} = stress intensity factor of Mode II crack;

K_{IIC} = fracture toughness for Mode II cracks;

SIF = stress intensity factor;

t = coordinate of a point on crack surface;

Y_{II} = dimensionless K_{II};

UCS = uniaxial compressive strength;

α = the angle between crack and the σ_3-axis;

α_{m} = orientation of the most unfavorable crack;

$\Phi(z), \Omega(z)$ = complex stress functions;

$\varphi(z) = \int \Phi(z)\mathrm{d}z;\ \omega(z) = \int \Omega(z)\mathrm{d}z;$

$\kappa = (3 - \nu)/(1 + \nu)$ for plane stress and $\kappa = 3 - 4\nu$ for plane stress;

σ_{f} = crack surface friction;

σ_{N} = normal compressive stress acting on crack surface;

σ_{S} = shear stress which is parallel to crack surface;

σ_{U} = uniaxial compressive strength for specimens containing collinear cracks.

$X(z)$ = Plemelj function.

Acknowledgement. This work has been funded in part by NSFC-50639100 and by Science and Technology Funding of Sichuan 2008JY0041.

REFERENCES

[1] Nemat-Nasser, S. and Horii, H. Compression-induced nonplanar crack extension with application to splitting, exfoliation, and rockbust. *Journal of Geophysical Research,* 87(B8), 6805–6821 (1982).

[2] Steif, P. S. Crack extension under compressive loading. *Engineering and Fracture Mechanics,* 20, 463–473 (1984).

[3] Ashby, M. F. and Hallam, S. D. The failure of brittle solids containing small cracks under compressive stress states. *Acta Metallica,* 34, 497–510 (1986).

[4] Li, C. and Nordlund E. Deformation of brittle rocks under compression with particular reference to microcracks. *Mechanics of Materials,* 15, 223–239 (1993).

[5] Germanovich, L. N., Salganik, R. L., Dyskin, A. V. and Lee, K. K. Mechanisms of brittle fracture of rock with pre-existing cracks in compression. *PHGEOPH,* 143, 117–147 (1994).

[6] Baud, P., Reuschle, T. and Charleg, P. An improved wing crack model for the deformation and failure of rock in compression. *International Journal of Rock Mechanics and Mineral Science Geomechanics,* 33, 539–542 (1996).

[7] Rice, J. R., Lapusta, N. and Ranjith, K. Rate and state dependent friction and the stability of sliding between elastically deformable solids. *Journal of Mechanics and Physics of Solids,* 49, 1865–1898 (2001).

[8] Newman, J. C. An improved method of collocation for the stress analysis of cracked plate with various shaped boundaries. *NASA TN D-6376,* 1971.

[9] Zhu, Z., Wang, L., Mohanty, B. and Huang, C. Stress intensity factor for a cracked specimen under compression. *Engineering and Fracture Mechanics,* 73, 482–489 (2006).

[10] Zhu, Z. New biaxial failure criterion for brittle materials in compression. *Journal of Engineering Mechanics,* 125, 1251–1258 (1999).

[11] Zhu, Z., Ji, S. and Xie, H. An improved method of collocation for the problem of crack surface subjected to uniform load. *Engineering and Fracture Mechanics,* 54, 731–741 (1996).

[12] Zhu, Z., Xie, H. and Ji, S. The mixed boundary problems for a mixed mode crack in a finite plate. *Engineering and Fracture Mechanics,* 56, 647–655 (1997).

[13] Zhu, Z. and Xie, H. Calculation method of the SIF and COD for crack surfaces subjected to uniform loading. *Journal of Computing and Structural Mechanics Applications,* 14, 182–188 (1997).

[14] Xie, H., Zhu, Z. and Fan T. The analysis of rock fracture properties by using boundary collocation method. *Acta Mechanica Sinica,* 30, 238–246 (1998).

[15] Willmore, T. J. The distribution of stress in the neighborhood of a crack. *Quarterly Journal of Mechanics and Applied Mathematics,* 2, 53 (1949).

[16] Muskelishvili, N. I. *Some Basic Problems of Mathematical Theory of Elasticity,* Noordhoff, Amsterdam, 1953.

[17] Mikhlin, S. G. Integral Equations, p. 205, Pergamon, Oxford, 1957.

[18] Erdogan, F. On the stress distribution in plates with collinear cuts under arbitrary loads, in *Proceedings of the 4th U.S. National Congress of Applied Mechanics,* Vol. 1, pp. 547–553, American Society of Mechanical Engineers, New York, 1962.

[19] Hori, M. and Nemat-Nasser, S. Interacting micro-cracks near the tip in the process zone of a macrocrack. *Journal of Mechanics and Physics of Solids,* 35, 601–629 (1987).

[20] Gong, S. X. Microcrack interaction with a finite main crack: an exact formulation. *International Journal of Fractures,* 66, 51–66 (1994).

[21] Wang, R. D. The stress intensity factors of a rectangular plate with collinear cracks under uniaxial tension. *Engineering and Fracture Mechanics,* 56, 347–356 (1997).

[22] Chen, Y. Z., Hasebe, N. and Lee, K. Y. *Multiple Crack Problems in Elasticity,* WIT Press, Southampton, 2003.

[23] England, A. H. Complex Variable Methods in Elasticity, Wiley-Interscience, New York, 1971.

[24] Milne-Thomson, L. M. Elliptic integrals, Chapter 17 in *Handbook of Mathematical Functions with Formulas, Graphs, and Mathematical Tables,* pp. 589–626, ed. M. Abramowitz and I. A. Stegun, National Bureau of Standards, Washington, DC, 1968.

[25] Lee, S. and Ravichandran, G. Crack initiation in brittle solids under multiaxial compression. *Engineering and Fracture Mechanics,* 70, 1645–1658 (2003).

[26] Jaeger, J. C. Failure and breakage of rocks. Brittle fracture of rocks, in *Proceedings of the 8th Symposium on Rock Mechanics,* Baltimore, pp. 3–57, 1967.

[27] Andreev, G. E. *Brittle Failure of Rock Materials,* Balkema, Rotterdam, 1995.